Red Emissive Two-Photon Probe for Real-Time Imaging of Mitochondria Trafficking

ARTICLE *in* ANALYTICAL CHEMISTRY · JUNE 2014

Impact Factor: 5.64 · DOI: 10.1021/ac5014805 · Source: PubMed

6 AUTHORS, INCLUDING:

Avik Ranjan Sarkar
Ajou University
19 PUBLICATIONS **299** CITATIONS

SEE PROFILE

analytical chemistry

Letter

pubs.acs.org/ac

Red Emissive Two-Photon Probe for Real-Time Imaging of Mitochondria Trafficking

Avik R. Sarkar,[†,§] Cheol Ho Heo,[†,§] Hyo Won Lee,[†] Kyung Hee Park,[‡] Young Ho Suh,[‡] and Hwan Myung Kim*[,†]

[†]Department of Energy Systems Research, Ajou University, Suwon, Gyeonggi-do 443-749, Korea

[‡]Division of Pharmacology, Department of Biomedical Sciences, Ajou University School of Medicine, Suwon, Gyeonggi-do 443-721, Korea

Supporting Information

ABSTRACT: Mitochondria trafficking plays an essential role for supplying energy in the neuronal system. We report here a red emissive two-photon probe for mitochondria (CMT-red) that showed high selectivity and robust staining ability for mitochondria, high photostability under a two-photon microscopy imaging condition, and low cytotoxicity. This probe can be easily loaded into live cells and tissue and used for real-time, high resolution imaging of the mitochondria trafficking in primary cortical neurons as well as in rat hippocampal tissue.

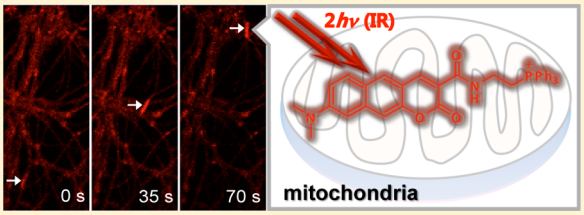

Among the cellular organelles, mitochondria are a major target to study human physiology and diseases because they perform many functions and have numerous proteins responsible for oxidative phosphorylation.[1] Indeed, the defects of mitochondrial function could be directly related to aging, cancer, and neurodegenerative disorders including Alzheimer's, Huntington's, and Parkinson's diseases.[2] In mammalian brain, about 20% of resting metabolic energy is dedicated to maintaining continuous neuronal function.[3] As such, the transport of mitochondria in the neuronal system plays an important role for supplying energy, while mitochondrial morphology continuously undergoes remodeling through biogenesis, fission, fusion, and autophagy.[4] To understand the biological and pathological roles of mitochondria, it is crucial to monitor mitochondria dynamics in real-time at the subcellular level.

The use of small molecule fluorescent probes has become a powerful tool in molecular imaging studies because these compounds exhibit less steric bulk, have faster rates of labeling, and do not require transfection.[5,6] Two-photon microscopy (TPM) uses two near IR and low energy photons as the excitation light, which provides advantages such as greater tissue penetration, localization of the excitation, and longer observation times.[7] In combination with TPM, red emissive fluorescent probes are attractive for imaging in live cells and tissues, because they have better spectral separation from cellular absorption and autofluorescence than probes that emit in the blue to yellow fluorescence range, thereby enhancing the contrast between the readout and background emission.[8,9] As the red emissive probes for mitochondria, π-extended cyanine derivatives such as MitoTracker Red FM (MTR, Scheme 1) have been most frequently used.[10] However, these probes suffer from photobleaching and/or small Stokes shift, so that real-time imaging studies in high resolution are compromised. Therefore, there is a strong need for development of a red emissive and photostable TP probe for mitochondria.

Scheme 1. Structures of CLT-yellow, CMT-red (1), and MTR

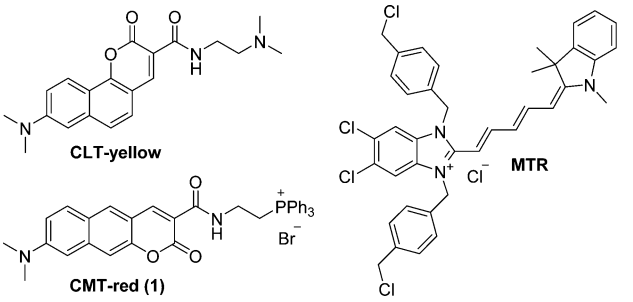

Recently, we reported a 2*H*-benzo[*h*]chromene-2-one derived TP probe for lysosomes (CLT-yellow, Scheme 1),[11] which showed an emission maximum at 580 nm in buffer solution. We anticipated that a system with greater linear π-conjugation than that of CLT-yellow would display enhanced intramolecular charge transfer (ICT), thereby shifting the emission maximum to the red region. In addition, higher photostability than MTR can be achieved by incorporating a C=C conjugated bridge within the cycle, because the open chain analogue could undergo photochemical instability such as photoisomerization of the C=C bond.[12] Herein, we report a red color emissive and photostable TP probe for mitochondria

Received: April 22, 2014
Accepted: May 31, 2014

   dx.doi.org/10.1021/ac5014805 | *Anal. Chem.* XXXX, XXX, XXX–XXX

(CMT-red, **1**, Scheme 1), derived from an electron donor–acceptor substituted 2*H*-benzo[*g*]chromene-2-one as the fluorophore and a triphenylphosphonium salt (TPP) as the mitochondrial-targeting site.[13]

The synthetic procedure of **1** is described in the Supporting Information. The solubility of **1** in phosphate buffer saline (10 mM PBS, pH 7.4) was approximately 6 μM, which was sufficient to stain the cells (Figure S1, Supporting Information). Under these conditions, this probe exhibited an absorption and emission maximum at 470 nm (ε = 1.25 × 10^4 M^{-1} cm^{-1}) and 626 nm (Φ = 0.07), respectively, with a large Stokes shift of 156 nm (Figure 1a). The fluorescence lifetime of **1** was 1.12 ns

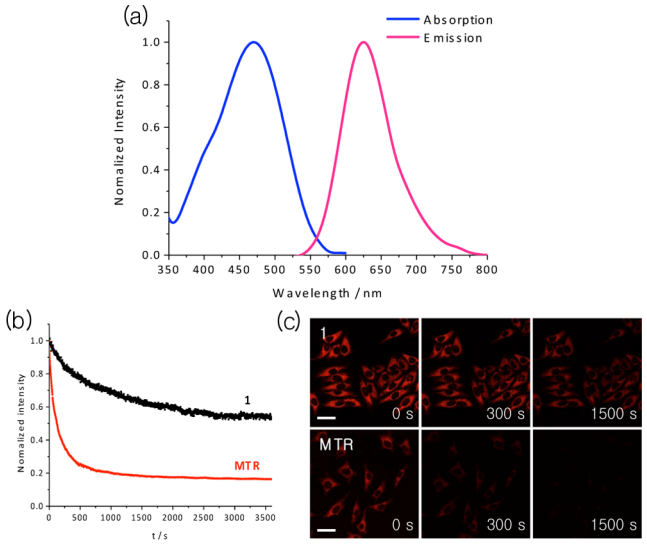

Figure 1. (a) One-photon absorption and emission spectra (normalized) of **1** in PBS buffer (10 mM, pH 7.4). (b) Two-photon excited fluorescence intensity (normalized) of **1** and MTR as a function of time acquired from **1**-labeled (0.5 μM) and MTR-labeled (1 μM) HeLa cells. The digitized intensity was recorded with 2.00 s intervals for the duration of 1 h using *xyt* mode (λ_{ex} = 820 nm) with femtosecond pulses. (c) Corresponding TPM images of (b) at 0, 300, and 1500 s, respectively. Cells shown are representative images from replicate experiments (n = 5). Scale bar: 45 μm.

(Figure S2, Supporting Information). The emission maximum of **1** is more than 40 nm red-shifted from that of CLT-yellow (580 nm). These changes can be attributed to the greater stabilization of the charge-transfer excited state in **1**, which would enhance ICT. Further, **1** is pH insensitive in the biologically relevant pH range (Figure S3, Supporting Information). The two-photon action cross section values ($\Phi\delta_{max}$) of **1** were determined to be 50 and 20 GM in dioxane and EtOH, respectively (Figure S4, Supporting Information). These values are comparable to that of CLT-yellow (47 GM in EtOH).[11] Further, the TPM images of the **1**-labeled cells and tissues were bright at 600–700 nm (Figures 2–4).

To demonstrate the utility of **1** as a marker for mitochondria, a colocalization experiment was investigated in different cell lines. Human Caucasian glioblastoma T98G cells were colabeled with **1** and MitoTracker Green (MTG), a well-known green emissive marker for mitochondria.[10] The TPM image of **1** merged well with the MTG image (Figure S6, Supporting Information). The Pearson's colocalization coefficient (A) of **1** and MTG was 0.96 ± 0.05 as calculated using LAS AF software, indicating that **1** existed predominantly in the mitochondria. Similar results were obtained in HeLa cells and primary cultured cortical neurons (Figure S6, Supporting Information).

We then performed photobleaching studies with **1** in cells in comparison to MTR. Upon excitation at 820 nm with femtosecond pulses at 1.5 mW average power at the focal plane, the two-photon excited fluorescence (TPEF) intensity was collected for 1 h with 2.00 s intervals. Figure 1c revealed that the TPM image of MTR labeled cells returned to the dark state within 300 s, whereas cells labeled with **1** retained more than 50% of initial intensity after 1 h (Figure 1b). Further, the half-lives for the decay of TPEF intensity during 1 h were 1224 and 97 s for **1** and MTR, respectively (Figure S7, Supporting Information).[12] The higher photostability of **1** than MTR is likely due to the structural motif that encloses the conjugated double bond within a ring. Moreover, **1** showed low cytotoxicity as determined using a MTS assay (Figure S8, Supporting Information).

We next evaluated the staining ability of **1** in comparison to MTR. The mitochondrial membrane potential ($\Delta\Psi_m$) is an important parameter for mitochondrial physiology.[13] To assess whether **1** could stain mitochondria in live cells if the $\Delta\Psi_m$ was altered, T98G cells were pretreated with CCCP (carbonyl cyanide *m*-chlorophenylhydrazone) prior to being labeled with **1** or MTR (Figure S9, Supporting Information). CCCP promotes the release of intramitochondrial cations and causes rapid acidification by collapsing the mitochondrial $\Delta\Psi_m$.[14] When the cells were treated with 25 μM CCCP, **1** remained unaltered in its staining ability and specificity for mitochondria after treatment with CCCP (Figure S9a,b, Supporting Information), whereas MTR no longer persisted in mitochondria and accumulated in the cytoplasm (Figure S9c, Supporting Information). Further, TPM images clearly showed that the tubule-like mitochondria adopted a globular morphology upon the treatment with CCCP. To confirm these observations, we conducted colocalization experiments with pEYFP-Mito, a yellow fluorescence protein for mitochondria, and **1** or MTR in T98G cells (Figure 2). It is well-known that the staining ability of pEYFP-Mito does not depend on the mitochondrial $\Delta\Psi_m$.[15] The A values between the TPM image of **1** and the OPM image of pEYFP-Mito were nearly the same whether the cells were pretreated with CCCP or not (A = 0.97 and 0.96, respectively, Figure 2). However, under similar experimental conditions, the A value was significantly reduced for MTR. These results establish that **1** can serve as a TP probe for mitochondria in live cells.

The abilities of **1** to function in real-time imaging were then tested in primary cultured cortical neurons. The rapid transport of tubule-like mitochondria along the dendrites and axons was clearly visualized in neurons (Figure 3). Moreover, variations in the speed and direction of their movements were detected along with their morphological activity (Video S1, Supporting Information). As expected, we were unable to obtain moving images using MTR under similar conditions due to its rapid photobleaching. This outcome clearly demonstrated the utility of **1** as a TP probe for real-time imaging of mitochondrial trafficking.

We further investigated the utility of **1** in tissue imaging. TPM images were obtained from a slice of two-week old rat hippocampal tissue incubated with **1** for 1 h at 37 °C. As the structure of the brain tissue is known to be inhomogeneous throughout its entire depth, we obtained 100 TPM images at depths of 90–200 μm. The accumulated image revealed that

dx.doi.org/10.1021/ac5014805 | *Anal. Chem.* XXXX, XXX, XXX–XXX

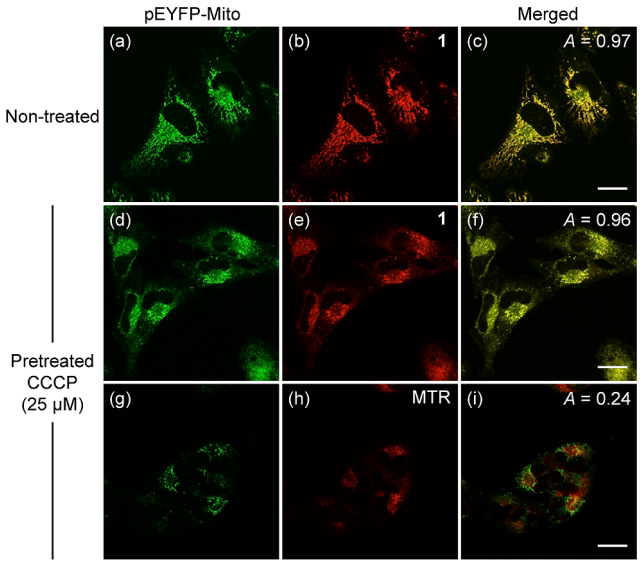

Figure 2. OPM, TPM, and merged images of T98G cells colabeled with pEYFP-Mito and **1** (a–f), and pEYFP-Mito and MTR (g–i), before and after pretreatment with 25 μM CCCP for 8 h. The wavelengths for OP excitation were 488 nm (pEYFP-Mito) and 514 nm (MTR FM) and for TP excitation was 820 nm (**1**); the emissions were collected at 500–550 nm (pEYFP-Mito), 600–700 nm (**1**), and 650–700 nm (MTR). The images shown are representative of the images obtained in repeat experiments (n = 5). Scale bars: 25 μm.

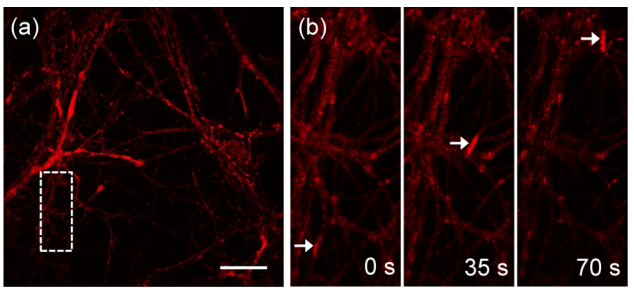

Figure 3. TPM images of primary cultured cortical neurons labeled **1** for 30 min at 37 °C. (a) Images at 100× magnification. (b) Enlargement of the white box in (a) showing the transport of mitochondria along the neurons. The excitation wavelength was 820 nm, and the corresponding emission was collected at 600–700 nm. The images shown are representative of the images obtained in repeat experiments (n = 3). Scale bar: 20 μm.

mitochondria were evenly distributed in the CA1-CA3 region (Figure 4a). Moreover, the image taken at higher magnification and their 3D constructed images allowed the visualization of the individual mitochondria in the pyramidal neuronal layer of the CA1 region (Figure 4b,c). Hence, **1** is clearly capable of visualizing the mitochondria at a depth of more than 200 μm in live tissue by TPM.

In conclusion, we have developed a red-emissive and photostable TP fluorescence probe for mitochondria (CMT-red, **1**). This probe showed high selectivity and robust staining ability for mitochondria and low cytotoxicity and pH insensitivity in the biologically relevant pH range. This probe can be easily loaded into the live cells and tissue and used for real-time, high resolution imaging of the mitochondria trafficking in primary cortical neurons as well as in rat hippocampal tissue. These findings demonstrate that this

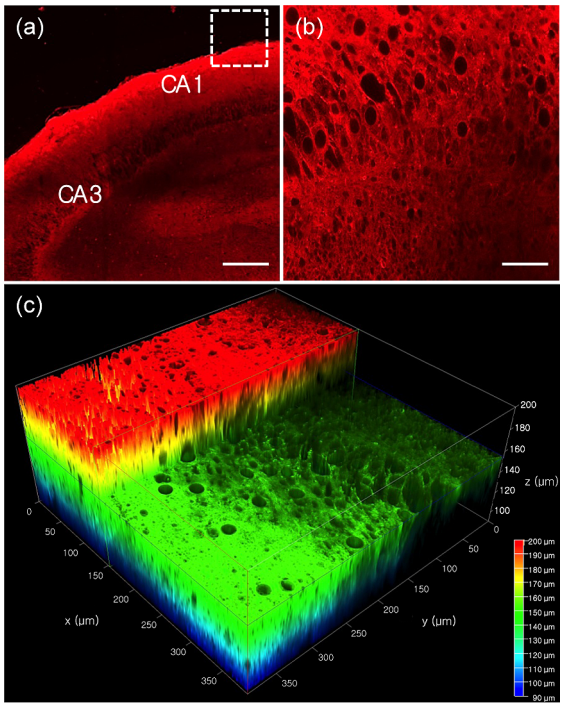

Figure 4. Images of a rat hippocampal slice stained with **1** for 1 h at 37 °C. (a) TPM image of the CA1 and CA3 regions. (b) Enlarged images of the white box in (a) at a depth of 150 μm with 40× magnification. (c) 3D reconstructed TP images of the CA1 region. 100 TPM images were accumulated along the z direction with 40× magnification at depths of 80–200 μm from the surface of the hippocampal slice. The TPEF was collected at 600–700 nm upon excitation at 820 nm with femtosecond pulse. Scale bars: (a) 300 μm and (b) 60 μm. The images shown are representative of the images obtained in repeat experiments (n = 5).

probe may find useful applications in biomedical research through the use of TPM.

■ ASSOCIATED CONTENT

Ⓢ Supporting Information

Additional figures (Figures S1–S11) and Video S1. This material is available free of charge via the Internet at http://pubs.acs.org.

■ AUTHOR INFORMATION

Corresponding Author

*E-mail: kimhm@ajou.ac.kr.

Author Contributions

§A.R.S. and C.H.H. contributed equally.

Notes

The authors declare no competing financial interest.

■ ACKNOWLEDGMENTS

This work was supported by National Research Foundation (NRF) grants funded by the Korean Government (2011-0028663) and Priority Research Centers Program through the NRF (2009-0093826).

■ REFERENCES

(1) Baines, C. P. *Annu. Rev. Physiol.* **2010**, *72*, 61.

(2) (a) Turrens, J. F. *J. Physiol.* **2003**, *552*, 335. (b) Dickinson, B. C.; Chang, C. J. *Nat. Chem. Biol.* **2011**, *7*, 504. (c) Chang, D. T.; Reynolds, I. J. *Prog. Neurobiol.* **2006**, *80*, 241.

dx.doi.org/10.1021/ac5014805 | *Anal. Chem.* XXXX, XXX, XXX–XXX

(3) Silver, I.; Erecinska, M. *Adv. Exp. Med. Biol.* **1998**, *454*, 7.
(4) (a) Chang, D. T.; Honick, A. S.; Reynolds, I. J. *J. Neurosci.* **2006**, *26*, 7035. (b) Rube, D. A.; van der Bliek, A. M. *Mol. Cell. Biochem.* **2004**, *256*−*257*, 331. (c) Peterson, C. M.; Johannsen, D. L.; Ravussin, E. *J. Aging Res.* **2012**, *2012*, 194821.
(5) (a) Chan, J.; Dodani, S. C.; Chang, C. J. *Nat. Chem.* **2012**, *4*, 973. (b) Lavis, L. D.; Raines, R. T. *ACS Chem. Biol.* **2008**, *3*, 142. (c) Kim, H. N.; Lee, M. H.; Kim, H. J.; Kim, J. S.; Yoon, J. *Chem. Soc. Rev.* **2008**, *37*, 1465.
(6) (a) Kim, H. M.; Cho, B. R. *Acc. Chem. Res.* **2009**, *42*, 863. (b) Kim, H. J.; Heo, C. H.; Kim, H. M. *J. Am. Chem. Soc.* **2013**, *135*, 17969. (c) Bae, S. K.; Heo, C. H.; Choi, D. J.; Sen, D.; Joe, E. H.; Cho, B. R.; Kim, H. M. *J. Am. Chem. Soc.* **2013**, *135*, 9915. (d) Heo, C. H.; Kim, K. H.; Kim, H. J.; Baik, S. H.; Song, H.; Kim, Y. S.; Lee, J.; Mookjung, I.; Kim, H. M. *Chem. Commun.* **2013**, *49*, 1303.
(7) (a) Zipfel, W. R.; Williams, R. M.; Webb, W. W. *Nat. Biotechnol.* **2003**, *21*, 1369. (b) Helmchen, F.; Denk, W. *Nat. Methods* **2005**, *2*, 932.
(8) Weissleder, R.; Ntziachristos, V. *Nat. Med.* **2003**, *9*, 123.
(9) Zhang, X.; Xiao, Y.; Qu, J.; Kim, B.; Yue, X.; Belfield, K. D. *J. Org. Chem.* **2013**, *78*, 9153.
(10) Haugland, R. P., Ed. The Molecular Probes Handbook: A Guide to Fluorescence Probes and Labeling Technologies, 10th ed.; Molecular Probes: Eugene, OR, 2005.
(11) Son, J. H.; Lim, C. S.; Han, J. H.; Danish, I. A.; Kim, H. M.; Cho, B. R. *J. Org. Chem.* **2011**, *76*, 8113.
(12) Kim, H. M.; Yang, W. J.; Kim, C. H.; Park, W. H.; Jeon, S. J.; Cho, B. R. *Chem.—Eur. J.* **2005**, *11*, 6386.
(13) (a) Murphy, M. P.; Smith, R. A. *Annu. Rev. Pharmacol. Toxicol.* **2007**, *47*, 629. (b) Kelso, G. F.; Porteous, C. M.; Coulter, C. V.; Hughes, G.; Porteous, W. K.; Ledgerwood, E. C.; Smith, R. A.; Murphy, M. P. *J. Biol. Chem.* **2001**, *276*, 4588. (c) Yousif, L. F.; Stewart, K. M.; Kelley, S. O. *ChemBioChem* **2009**, *10*, 1939.
(14) Caporale, T.; Ciavardelli, D.; Di Ilio, C.; Lanuti, P.; Drago, D.; Sensi, S. L. *Exp. Neurol.* **2009**, *218*, 228.
(15) Kim, E. H.; Sohn, S.; Kwon, H. J.; Kim, S. U.; Kim, M. J.; Lee, S. J.; Choi, K. S. *Cancer Res.* **2007**, *67*, 6314.

dx.doi.org/10.1021/ac5014805 | *Anal. Chem.* XXXX, XXX, XXX−XXX